Contents lists available at ScienceDirect

Int J Appl Earth Obs Geoinformation

Four decades of land cover and forest connectivity study in Zambia—An object-based image analysis approach

Darius Phiri[*], Justin Morgenroth, Cong Xu

New Zealand School of Forestry, University of Canterbury, Christchurch, New Zealand

ABSTRACT

Land cover dynamics in the tropical dry environments of sub-Saharan Africa are not well understood compared to humid environments, especially on a national scale. Previous studies describing land cover in the dry tropics are spatially or temporally constrained. This study presents the first long-term (1972–2016) nationwide land cover dynamics and forest connectivity analyses for Zambia. We employed 300 Landsat images and an object-based image analysis (OBIA) approach with the Random Forests (RF) classifier to map nine land covers at six time steps (1972, 1984, 1990, 2000, 2008 and 2016). Post-classification change detection was used to understand the dynamics, while landscape metrics were derived to assess the forest structural connectivity. Overall accuracies ranging from 79 to 86% were achieved. In 1972, 48% of Zambia was covered by primary forest and 16% was covered by secondary forest. By 2016, 62.74% of Zambia had undergone changes, with primary forest decreasing by 32% and secondary forest increasing by 23%. Our results showed that forests have been recovering by 0.03 to 1.3% yr^{-1} (53, 000–242, 000 ha yr^{-1}); however, these rates are markedly lower than deforestation rates (- 0.54 to - 3.05% yr^{-1}: 83, 000–453, 000 ha yr^{-1}). Annual rates of change varied by land cover, with irrigated crops having the largest increase (+ 3.19 yr^{-1}) and primary forest having the greatest decrease (-2.48% yr^{-1}). Forest connectivity declined by 22%, with primary forest having the greatest decline, while the connectivity for secondary and plantation forest increased. We showed here that land cover in Zambia is highly dynamic with high rates of change, low forest recovery and decline in forest connectivity. These findings will aid in land use planning, reporting for the forthcoming 2020 Global Forest Resources Assessment, and carbon accounting, especially under the reduction in carbon emissions from deforestation and degradation programme (REDD +).

1. Introduction

Tropical dry environments are of significant importance to global carbon and biodiversity, but are often overlooked relative to tropical humid environments (Ernst et al., 2013; Kalacska et al., 2007). Comprising approximately 14% of global forests, tropical dry environments are among the areas which are being rapidly transformed by landuse and climate change. Although previous studies have mapped land cover on regional and global scales (Chen et al., 2015; Hansen et al., 2013), land cover dynamics and forest connectivity in these areas are not well understood on a national scale because studies are temporally constrained (Cao et al., 2015; Mayes et al., 2015). In subSaharan Africa, rapidly increasing populations have increased the demand for natural resources such as land for both agriculture and settlements (Hansen et al., 2000). Climate change and the expansion of agricultural and urban land uses has had a negative impact on the quality and quantity

of other natural land covers such as forests, wetlands and water bodies (Brandt et al., 2018; Dronova et al., 2012). These land use and land cover changes affect biodiversity through landscape fragmentation and loss of structural connectivity, especially in forest areas (Grech et al., 2018; Piquer-Rodríguez et al., 2015). Structural connectivity, which is the spatial relationship among the elements of the landscape, is a key topic in forest resilience, gene flow and habitat provision (Fagan et al., 2016; Henry et al., 2018). Therefore, understanding land cover dynamics and forest connectivity on a national scale is critical for land use planning and implementation of conservation strategies (Eberle et al., 2017; Haddad et al., 2015).

National-scale information on the condition and quantity of varying land covers is also important for effective policy formulation for the sustainable management of natural resources and understanding the uncertainties resulting from climate change (Dronova, 2015; Uddin et al., 2015). However, such critical information on land cover is
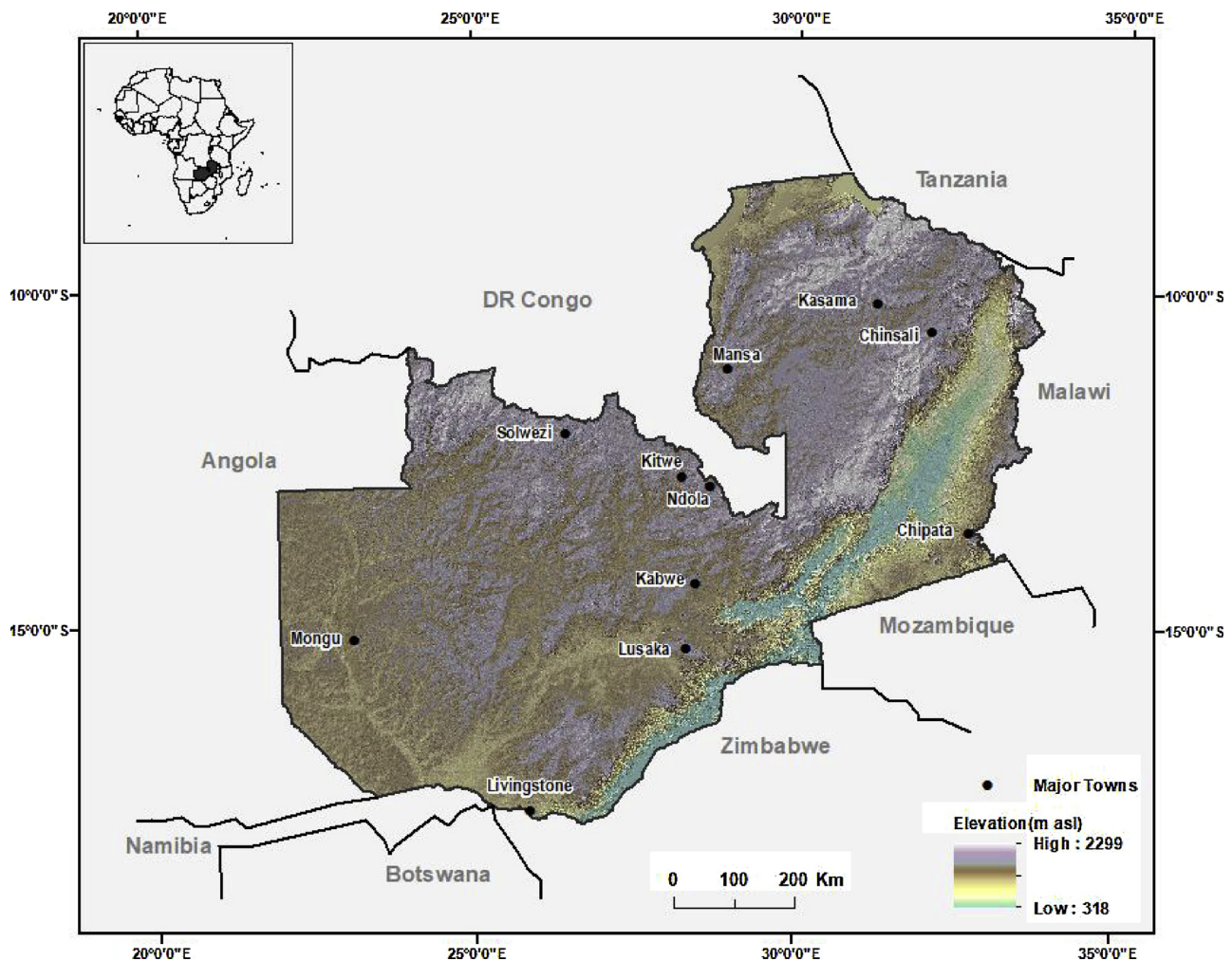
Fig. 1. The location of the study area, Zambia, and the elevation across the country as a hillshade model.

lacking in most dry-tropical subSaharan countries (De Sy et al., 2012; Gilani et al., 2015; Kindu et al., 2013). Ernst et al. (2013) reported that most of the data on land cover for Africa is available through the Food and Agriculture Organisation (FAO); however, the data lacks consistency and is usually spatially and temporally incomplete, hence it is of limited use. The lack of basic data such as detailed historical land cover maps confirms the reports by the Intergovernmental Panel on Climate Change (IPCC) which recognised sub-Saharan African countries such as Zambia as data deficit areas (De Sy et al., 2012). This draws attention to the need for national-scale land cover information, dating back several decades in order to understand historic land cover changes, present land cover status, and to inform future land cover trends.

Like many other sub-Saharan countries, the Zambian landscape has a high rate of deforestation which has led to landscape fragmentation and loss of biodiversity value (Syampungani et al., 2016). As a result of this, Zambia was selected as one of the pilot countries for the United Nations (UN) reducing emissions from deforestation and forest degradation (UN-REDD +) initiative in 2010 (Leventon et al., 2014). In addition to deforestation, forest degradation which results from unsustainable utilisation of natural resources is also a major issue (Syampungani et al., 2009). In rural areas where shifting cultivation is practised, land is usually left fallow after 3–5 years of cultivation which leads to degraded forests regenerating into secondary forests. This process of forest regeneration combined with other restoration programmes result in forest recovery in some areas (Müller et al., 2016; Schulz et al., 2010). Together, deforestation, forest degradation, and

recovery result in a dynamic landscape which requires frequent national-scale mapping and description in order to be fully understood (Barbosa et al., 2014).

Advancements in satellite remote sensing technology in the last four decades make it possible to monitor the Earth's surface with a high degree of certainty (Finer et al., 2018). The availability of Landsat imagery coupled with machine-learning analysis presents opportunities for large-area land cover mapping (Belgiu and Drăguţ, 2016; Hansen, 2012). With the introduction of the free access policy in 2008 (Woodcock et al., 2008) and the long-term archive period dating back to 1972, Landsat data has become an important tool for long-term land cover monitoring at large spatial extents such as national or global scales (Hansen, 2012; Phiri and Morgenroth, 2017). Large-area land cover mapping using Landsat data has also been recognised as an important means for establishing baseline information for subsequent reporting and monitoring for climate change programmes. These programmes include the United Nations Framework Convention on Climate Change (UNFCCC), the Kyoto Protocol and the Paris Agreement under UN-REDD + initiative (De Sy et al., 2012; Ernst et al., 2013).

Remote sensing studies conducted in Zambia and other countries in sub-Saharan Africa to characterise land cover have either been conducted over relatively small extents (Munyati, 2000; Petit et al., 2001; Simwanda and Murayama, 2017) or short time period (Chomba et al., 2012; Mukosha, 2008). Consequently, there have been no studies focussing on national-scale land cover change in Zambia spanning more than a decade. Moreover, previous studies have focused more on quantifying forest losses without considering aspects of forest

connectivity and gains from forest regeneration. Information on forest connectivity has the potential to highlight the levels of landscape fragmentation - a major pathway to forest degradation. A long-term, national-scale land cover study is needed to describe forest cover dynamics and connectivity in Zambia.

To understand the different land cover dynamics in Zambia, we carried out a detailed spatial and multi-temporal analysis by quantifying land cover change and forest structural connectivity for six discrete time periods spanning from 1972 to 2016 using the freely available Landsat remotely sensed data. Specifically, we aimed to: (1) classify the area covered by different land covers, (2) determine the long-term land cover dynamics, and (3) quantify the forest connectivity by using different landscape metrics. The findings from this study will provide important information on the status of forests and land cover in general which is vital for national forest management and forest reference emission level (FREL) assessments for the UNREDD + .

2. Materials and methods

2.1. Study area

The study area covers the whole of Zambia, which is a sub-Saharan African country located in southern Africa between latitude 8 °S and 18 °S, and longitude 22 °E to 34 °E. Zambia is a landlocked country covering over 752,000 km^2 and sharing borders with Tanzania, Malawi, Mozambique, Zimbabwe, Angola and the Democratic Republic (DR) of Congo (Fig. 1). Zambia is characterised by a combination of both flat and mountainous areas, ranging from 318 m above sea level (asl) in the southern region to 2299 m asl in the northern region. The climate is subtropical with mean annual rainfall ranging from 800 to 1500 mm and mean annual temperature ranging from 5 to 35 °C (Phiri et al., 2016). Land covers including dry tropical secondary forests, grasslands and wetlands currently dominate the country.

According to the projections of the 2010 national census, Zambia has a population of about 17 million (annual growth rate of 3.2%) with a population density of 17 people km^{-2}, 65% of which live in rural areas and 35% in urban areas (Kalaba et al., 2013; Syampungani et al., 2010). The major socioeconomic activities include agriculture and mining. The Zambian landscape is under constant transformation due to shifting agriculture, mining and harvesting of forest resources and is ranked as one of the highest deforested countries in sub-Saharan Africa (Chidumayo, 2002, 2013).

2.2. Data sources

2.2.1. Remotely sensed data

This study used Landsat scenes with less than 10% cloud cover which were acquired from the United States Geological Survey (USGS). Landsat scenes were downloaded to temporally correspond to six time steps: 1972, 1984, 1990, 2000, 2008 and 2016. The time-steps were based on different socio-economic and political activities which had direct impacts on land cover and land use changes. These activities include the change of government in 1991, closing of mines between 1991 and 1996, and the economic recession in 2008 (Chidumayo, 2013). In this study, the September scenes for each time step were used because of the stability in the vegetation phenology, and high chances of acquiring cloudfree images. The whole study area is covered by 50 Landsat scenes (each scene 185 x 185 km), thus in total 300 scenes were processed for the six time steps. Four types of Landsat images (Table 1), including Multispectral scanner (MSS), Thematic mapper (TM), Enhanced thematic mapper (ETM +) and Observation land imager (OLI), were used in this study (see Phiri and Morgenroth (2017) for a detailed description of Landsat images). The images used were Landsat Level-1 products which are orthorectified and have high geometric accuracy (Chance et al., 2016; Young et al., 2017). All the Landsat ETM + and OLI-8 images were pansharpened to 15 m resolution. Six bands (three

Table 1
Description of the Landsat images used in this study.

Landsat Images	Year	Number Bands used	Radiometric Resolution (bit)	Spatial resolution (m)
MSS	1972/1984	4	6	60
TM	1990/2008	6	8	30
ETM +	2000	6	9	15
OLI	2016	6	12	15

Note that the spatial resolution of the ETM + and OLI images is 30 m; the images were pansharpened to 15 m.

visible and three infrared bands) were used for land cover classification on all the images, except for Landsat MSS, which has four bands.

The Shuttle Radar Topography Mission (SRTM) Digital Elevation Models (DEMs) generated by National Aeronautics and Space Administration (NASA), which have a spatial resolution of 30 m were used for topographic corrections. The SRTM DEMs were also downloaded from the USGS website. The DEMs, together with the Landsat data, were projected to a common projected coordinate system, World Geodetic System 84 (WGS 84), Zone 35 south.

2.2.2. Training and validation data

The training and validation datasets were derived by visual interpretation of the raw images. Random points were generated for the whole study areas and raw images were used to assign land covers classed by a trained assessor. Where possible, higher spatial resolution images in Google Earth (by employing a time lapse tool) were used to verify the interpreted land cover associated with each point, especially for the years after 2000 for which Google Earth has high spatial resolution images (e.g. SPOT and DigitalGlobe). The minimum number of sample points per land cover class were calculated based on the multinomial probability theory. (Chomba et al., 2012; Congalton and Green, 2009; Olofsson et al., 2014). According to the multinomial probability theory, a total of 5740 points were randomly generated across the whole country for each time step, thus six sets of random points were generated based on the year of analysis. The allocation of points to each class was done by using the estimated area of each land cover class from previous land cover products. The common practice in training and validation is to allocate more samples to training compared to validation (Congalton and Green, 2009; Olofsson et al., 2014). The samples were randomly allocated into training (70%–4020 samples) and validating samples (30%–1720 samples) following a ratio (70:30%) recommended by Phiri et al. (2018) and Gilbertson et al. (2017).

To understand the land cover transitions between forest and non-forest land covers, nine land covers were considered (see Supplementary Table 1). The non-forest classes included classes which have direct impacts on the forests (e.g. cropland, settlements, and irrigated crops), while three types of forests including primary, secondary and plantation forests were considered. Other natural land covers including grassland, wetland and water body were also included in the study. Primary forest represented undisturbed forests with closed canopy, while secondary forests represented forests under transition through disturbance and regeneration. The relationship between primary and secondary forest was central to the study because this relationship determines forest degradation, loss and recovery.

2.3. Methods

The steps used in the Landsat image analysis included pre-processing, segmentation, classification, post-classification change detection and forest connectivity analysis. The methods are described in detail below.

2.3.1. Pre-processing

Pre-processing improves the quality of the images by reducing errors associated with the image digital numbers (DN) resulting from atmospheric effects and surface irregularities. Previous studies have shown that preprocessing through atmospheric and topographic corrections improves the accuracy of Landsat imagery classification (Phiri et al., 2018; Vanonckelen et al., 2013; Young et al., 2017). In this study, atmospheric and topographic corrections were applied on each image using (moderate resolution atmospheric transmission) MODTRAN and cosine correction by transforming the DN values to the top of atmospheric (TOA) reflectance values. To reduce the misalignment between the images (Young et al., 2017), the Landsat MSS which were not perfectly aligned to the other images were registered to the 2016 Landsat OLI-8 images. The Landsat OLI-8 and ETM + were pan-sharpened to 15 m spatial resolution using panchromatic bands and the Pansharp algorithm in Geomatica PCI software (PCI Geomatics, Markham, Canada). Compared to other pansharpening techniques, the Pansharp algorithm reduces the errors resulting from image fusion (Gilbertson et al., 2017). The pansharpening technique fuses the high-resolution images (panchromatic bands) with low-resolution multi-spectral images in order to create enhanced high-resolution images. The high-resolution images preserve the colour from the original images while increasing the spatial resolution, and hence improving the classification accuracy (Gilbertson et al., 2017; Phiri et al., 2018).

2.3.2. Segmentation

Object-based image analysis (OBIA) groups pixels into homogeneous clusters through a process called segmentation, and has advantages over the traditional pixel-based approach (Myint et al., 2011). The multiresolution segmentation process in eCognition 9.3 (Trimble Navigation Ltd, Sunnyvale, California) was used to segment each Landsat scene independently. Multiresolution segmentation requires parameterisation of scale, shape and compaction. The scale parameter is critical as it determines the size of the segments. The Estimation of Segmentation Parameter (ESP) tool (Drăguţ et al., 2014; Drăguţ et al., 2010) was used to optimise the scale parameter. Once a scale was optimally selected, the shape and compaction parameters were changed iteratively and the resulting segmentations were visually assessed. The scale parameter ranged between 6 and 13, while shape and compaction were between 0.2 and 0.8 (see Supplementary Table 2). A weight of 1 was used for all the bands used in the multiresolution segmentation except for the NIR band, which was assigned a weight of 2 because it is important for discriminating vegetation (Gilbertson et al., 2017; Phiri et al., 2018).

2.3.3. Classification metrics and random forests classifier

Different input features were used during classification including those derived from spectral indices such as normalised difference vegetation index (NDVI), band values (TOA reflectance), texture values and geometry (Table 2). The features were chosen to separate similar land cover classes; for example, NDVI was important in separating vegetated from non-vegetated areas. Due to the differences in NIR spectral values between cropland and grassland, NIR was important in separating the two classes. Textural values are recommended for separating land covers with similar reflectance properties but different textural characteristics (Aguilar et al., 2016); hence, they were important in separating plantation forests from primary and secondary forests. Geometric features such as shape and length were vital in extracting classes with distinct shapes such as irrigated crops (Kindu et al., 2013).

Random forests (RF), a non-parametric machine-learning classifier, was applied on the segmented objects for classification because of its superior performance based on stability and efficiency on different sample sizes (Belgiu and Drăguţ, 2016). Higher accuracies have also been reported when RF was used for land cover classification as compared to other classifiers (Lebourgeois et al., 2017; Rodriguez-Galiano et al., 2012; Wieland and Pittore, 2014). RF generates a multitude of

decision trees based on subsamples (usually one-third of the total samples). Unlike traditional decision trees, which depend on a single decision tree, RF depends on the average of many decision trees which are generated using subsamples. Using a RF classifier requires setting two parameters, number of trees (Ntree) and number of features (Mtry). The Ntree was set to 500 and Mtry to the square root of the total number of features as recommended in previous studies (Belgiu and Drăguţ, 2016; Immitzer et al., 2016; Wieland and Pittore, 2014).

2.3.4. Accuracy assessment

The accuracy assessment of all the six (1972, 1984, 1990, 2000, 2008 and 2016) classified land cover maps was performed using the validation samples (30% of all the samples) derived from visual assessment of raw images as indicated in Section 2.2.2. Classification accuracy for each map was calculated using a confusion matrix by matching the validation samples and the thematic maps as recommended by Congalton and Green (2009). Statistics such as overall, producer's and user's accuracies were used to assess the classification accuracy. The overall accuracy was reported in order to determine the accuracy of the overall classification. Producer's and user's accuracy were also used to determine the class-level accuracy. In order to establish the reliability of the accuracy, the confidence interval for the overall accuracy was also calculated using Eq. (1) (Congalton and Green, 2009):

$$CI = p \pm (s \cdot Z1 - \alpha + \frac{1}{2n}) \tag{1}$$

where p is the user's, producer's or overall accuracy, s is the standard deviation, $Z_{1-\alpha}$ is the two-tailed normal score, and n is the total number of samples.

2.3.5. Change detection

To establish the magnitude of change between the six classification steps and for the whole period, 1972 to 2016, post-classification change detection was used by employing overlay tools under spatial analysis in ArcMap 10.4.1 (ESRI, 2016). Post-classification change detection is a comparative analysis which involves independently produced thematic maps (Schulz et al., 2010). This process involves combining the initial and the final map by taking into account the land cover classes assigned at each stage. Overlay tools including dissolving, merging and intersection were used to combine the maps and to derive important change information including the "to and from" change direction. The changes at each particular stage (i.e. 1972–1984; 1984–1990; 1990-200; 2000–2008; and 20082016) were first calculated, and then the change for the whole period (1972–2016) was established. Area and percentage change for each land cover were determined at each particular time step. To compare land cover percentages, especially for land covers with small areas (e.g. plantation forest, irrigated crops), the cover percentages were presented both as absolute values and also log base 10 ($\log_{10}$) transformations. Because $\log_{10}$ transformations for land cover percentages less than 1% resulted in a negative value, 1 was added to all land cover percentages (Eq. (2)):

$$LC_t = \log_{10}(LC_{orig} + 1) \tag{2}$$

where LC_t is the transformed land cover percentage and LC_{orig} is the untransformed land cover percentage. The rate of change for land covers was calculated using Eq. (3) (Gilani et al., 2015; Puyravaud, 2003):

$$r = \left(\frac{1}{t2 - t1}\right) x \ln(\frac{A1}{A2}) \tag{3}$$

where r is the rate of change, t_1 and t_2 are the years at the start (1) and the end (2) of the assessment, and A_1 and A_2 are the areas at the beginning (1) and at the end (2) of the assessment period. Positive values show an increase in land cover, while negative values show a decrease in land cover. Wall-to-wall land cover maps were also created for each

Table 2
Description of the features used for classification in the present study.

Type of Feature	Name	Description	References
Spectral information	Blue, Green, RED, NIR, SWIR1, SWIR2	Mean, maximum difference, inverse and standard deviation of the band values	Aguilar et al. (2016)
Spectral indices	Brightness	$\text{Brightness} = \frac{(\text{Red} + \text{Green} + \text{Blue})}{3}$	Bezryadin et al. (2007), Huete et al. (2002)
	Normalised Difference Vegetation Index (NDVI)	$\text{NDVI} = \frac{\text{NIR} - \text{Red}}{\text{NIR} + \text{Red}}$	
	Enhanced Vegetation index (EVI)	$\text{EVI} = 2.5 * \frac{(\text{NIR} - \text{Red})}{(\text{NIR} + 6 * \text{Red} - 7.5 * \text{Blue} + 1)}$	
	Green Atmospherically Resistant Index (GARI)	$\text{GARI} = \frac{\text{NIR} - [\text{Green} - 0.7(\text{Blue} - \text{Red})]}{\text{NIR} + [\text{Green} - 0.7(\text{Blue} - \text{Red})]}$	Gitelson and Merzlyak (1998)
	Leaf Area Index (LAI)	$\text{LAI} = (3.618 * \text{EVI} - 0.118)$	Atzberger et al. (2015)
	Mean visibility (MV)	$\text{MV} = \sqrt{\frac{\text{Blue} + \text{Green} + \text{Red}}{3}}$	
	Visible Atmospherically Resistant Index (VARI)	$\text{VAR} = \frac{\text{Green} - \text{Red}}{\text{Green} + \text{Red} - \text{Blue}}$	Gitelson et al. (2002)
	Soil adjacent total vegetation index (SATVI)	$\text{SATVI} = \frac{\text{SWIR} - \text{Red}}{\text{SWIR} + \text{Red}}(1 + 0.5) - \frac{\text{SWIR2}}{2}$	
	Soil Adjusted Vegetation Index (SAVI)	$\text{SAVI} = \frac{(\text{NIR} - \text{Red})}{(\text{NIR} + \text{Red})}(1 + L); \; L = 0.5$	
	Green Normalised Difference Vegetation Index (GNDVI)	$\text{GNDVI} = \frac{\text{NIR} - \text{Green}}{\text{NIR} + \text{Green}}$	
	Simple Ratio (SR)	$\text{SR} = \frac{\text{NIR}}{\text{Red}}$	Birth and McVey (1968)
	Burn Area Index (BAI)	$\text{BAI} = \frac{1}{(0.1 - \text{Red})^2 + (0.06 - \text{NIR})^2}$	Chuvieco et al. (2002)
	Difference Vegetation Index (DVI)	$\text{DVI} = \text{NIR} - \text{Red}$	Tucker (1979)
	Normalised Burn Ratio (NBR)	$\text{NBR} = \frac{(\text{NIR} - \text{SWIR})}{(\text{NIR} - \text{SWIR})}$	Key and Benson (2005)
	Normalised Ratio Vegetation Index (NRVI)	$\text{NRVI} = \frac{\text{RVI} - 1}{\text{RVI} + 1}$	Silleos et al. (2006)
Textural features	GLCM Homogeneity, GLCM Entropy, GLCM Agular second moment	GLCM based on standard deviation, mean values of bands and indices	Haralick and Shanmugam (1973)
Geometric features	Shape, width, area and length	Extent and characteristics of the segmented features	Wieland and Pittore (2014)

time step to visualise the distribution of land cover changes across all of Zambia.

The different stages of forest transition were identified based on the land cover change analysis. Five attributes of land cover transition including deforestation, forest degradation, afforestation, regeneration (regrowth) and forest recovery were evaluated (Chidumayo, 2013; McNicol et al., 2018). Deforestation was considered as the transition from forests to non-forests (GOFC-GOLD, 2009; McNicol et al., 2018); while degradation indicated changes from primary forest to secondary forest (Chidumayo, 2013). Afforestation was defined as the changes from non-forests to forests, and regeneration indicated the conversion of previously forested land to secondary forest and the growth of secondary forest to primary forest (Chidumayo, 1989). Finally, forest recovery comprised both afforestation and regeneration (Chidumayo, 2013; McNicol et al., 2018; Syampungani et al., 2016).

2.3.6. Forest connectivity

Forest connectivity was analysed using class-level landscape metrics based on patches from three forest classes: primary, secondary and plantation forest. Patches were defined as clusters of interconnected cell based on the 8-neighbour rule (Mc Garigal et al., 2012). The metrics were analysed as individual forest types and combined (all forests). The analysis was done using a spatial pattern analysis for categorical maps software, FRAGSTATS 4.1 (Mc Garigal et al., 2012).

Landscape metrics which best describe proximity and fragmentation were used to understand connectivity. The metrics calculated were Euclidean nearest neighbour distance (ENN), number of patches (NP), and connectivity (connectance) index (CI) (see Supplementary Table 3). ENN describes the proximity of different patches from neighbouring patches. NP describes the level of forest connectivity based on the number of patches for a specific classification time. CI presents probabilistic forest connectivity; it ranges from 0 to 1 or can be expressed as a percentage. CI models the relationship between patches by conducting a network analysis (Mc Garigal et al., 2012), and is calculated as:

$$\text{CI} = \left[\frac{\sum_{j \neq k}^{n} c_{ijk}}{\frac{n_i (n_i - 1)}{2}} \right] (100) \tag{4}$$

where CI is connectivity index, C_{ijk} is the connection between patch j and k of type i, and n_i is the number of patches for a specific class.

To establish the statistical significance and differences among the six classification periods, analysis of variance (ANOVA) was used for CI and ENN as they are continuous data. The Bonferroni test (Bonferroni, 1936), a post-hoc analysis, was also used to identify the years with different patterns. For NP, a Kruskal–Wallis non-parametric test (Kruskal et al., 1953) with Dunn's post-hoc test (Dunn, 1961) was used because NP is count data, which did not satisfy the normality of residuals assumption. All the statistical analyses were conducted in R statistical software (R Core Team, 2013).

3. Results

3.1. Land cover classification

Fig. 2 shows wall-to-wall land cover maps for Zambia for 1972, 1984, 1990, 2000, 2008 and 2016. The overall classification accuracy for the six time steps ranged from 79 to 86%, and the 95% confidence interval for the overall accuracies ranged between ± 3.31 and ± 3.79% (Table 3). The highest overall accuracy (86%) was from the 2016 map, while the lowest accuracy (79%) was from the 1972 map. It appears that the levels of accuracy were associated with the differences in spatial, spectral and radiometric resolution of the images used because the images with better properties had higher accuracies. Thus, the 60 m MSS for 1972 and 1984 had lower accuracies compared to the 30 m TM images for 1990, which had a lower overall accuracy compared to the 15 m ETM + and OLI-8 images.

The individual land cover accuracies (producer's and user's accuracies) were between 66 and 100%. Irrigated crops and water bodies had consistently high classification accuracies of nearly 100% across all
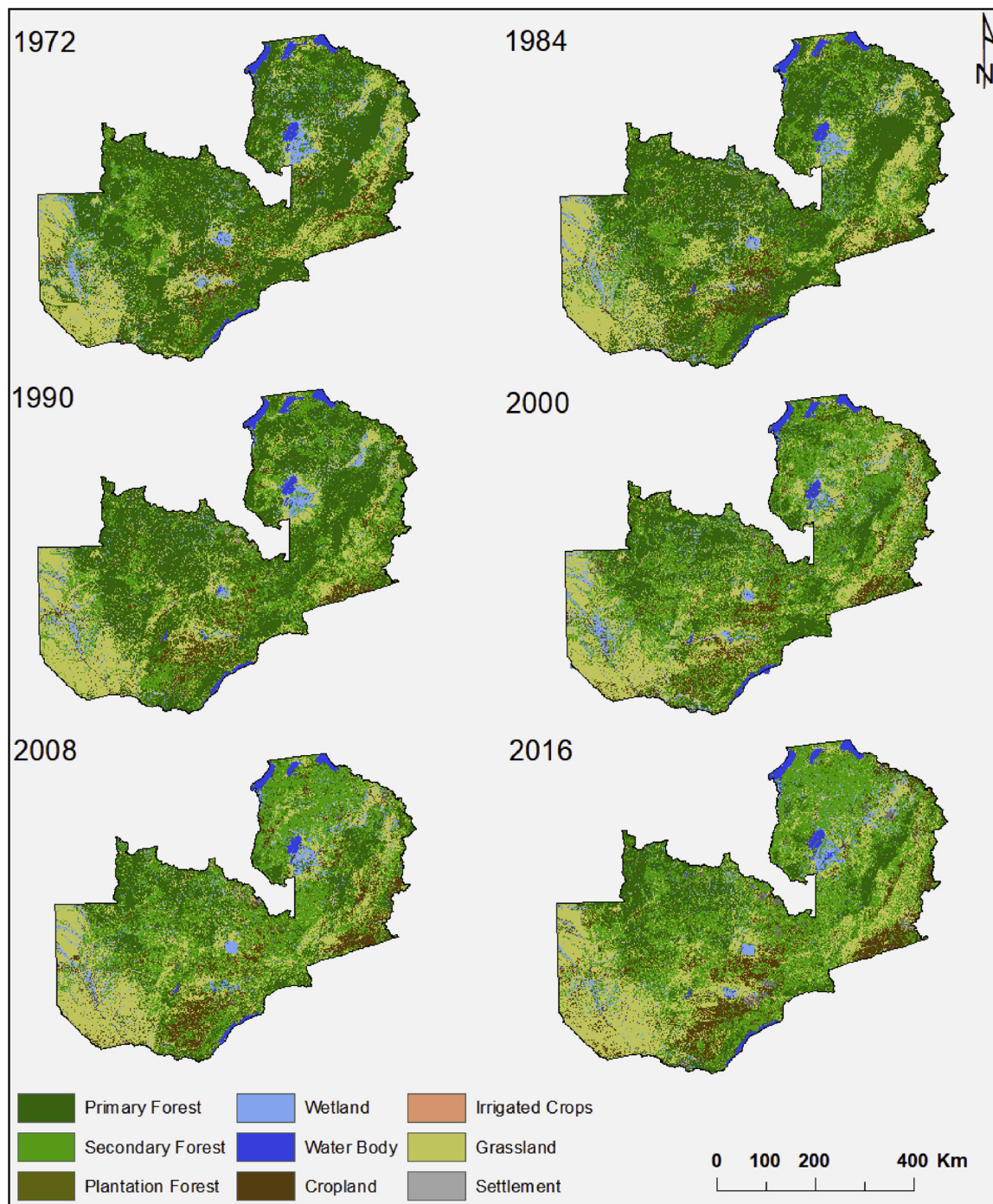
Fig. 2. Thematic land cover maps for Zambia for the six time steps between 1972 and 2016.

the maps. Primary and secondary forest had some of the lowest (66–67%) user's and producer's accuracy compared to other land cover classes, especially on 1972's Landsat MSS images (Table 3; see Supplementary Table 4).

3.2. Changes in land cover composition

Throughout the classification period, all the land cover classes were present; however, the area for individual land covers changed over time (Fig. 3). Between 1972 and 1990, primary forest was the dominant land cover with 48% (36,335,000 ha) which change to 41% (32,647,000 ha) before declining to 16% (12,434,000 ha) in 2016. Secondary forest had the highest coverage between 2000 and 2016, covering 35–38% of the

country. Between 1990 and 2000, a drastic change for primary and secondary forest was observed, with primary forest declining by 17% and secondary forest increasing by 14%. Although plantation forest and irrigated crops experienced some changes, they had the smallest (> 1%) area for all the years. Settlement area consistently increased from 0.54% (407,000 ha) in 1972 to 1.03% (773,000 ha) in 2016. Cropland increased from 6.16% in 1972 to 11.88% in 2016. Water body remained almost the same (1.70–1.80%) across the classification periods. By 2016, grassland increased by 4%, while wetland declined by 1% (Table 4).

Table 3
Overall, user's and producer's accuracy (in %) for the land cover classification with confidence intervals.

| Land cover	1972 PA	1972 UA	1984 PA	1984 UA	1990 PA	1990 UA	2000 PA	2000 UA	2008 PA	2008 UA	2016 PA	2016 UA
Primary forest	66	85	78	79	88	87	88	88	81	80	84	89
Secondary Forest	74	70	78	67	76	82	82	83	79	71	85	80
Plantation Forest	85	100	74	78	88	88	92	100	81	84	83	100
Wetland	88	73	90	80	79	82	79	88	85	85	84	85
Water body	100	100	86	98	93	95	93	99	100	98	100	98
Cropland	88	78	74	82	79	71	83	84	81	81	84	84
Irrigated Crops	91	100	91	100	83	94	100	100	98	94	100	97
Grassland	86	77	86	80	79	77	86	83	76	83	85	87
Settlement	76	92	77	98	75	76	78	80	85	82	93	83
Overall accuracy	79(± 3.79)		80(± 3.74)		82(± 3.63)		85(± 3.38)		81(± 3.70)		86(± 3.31)	
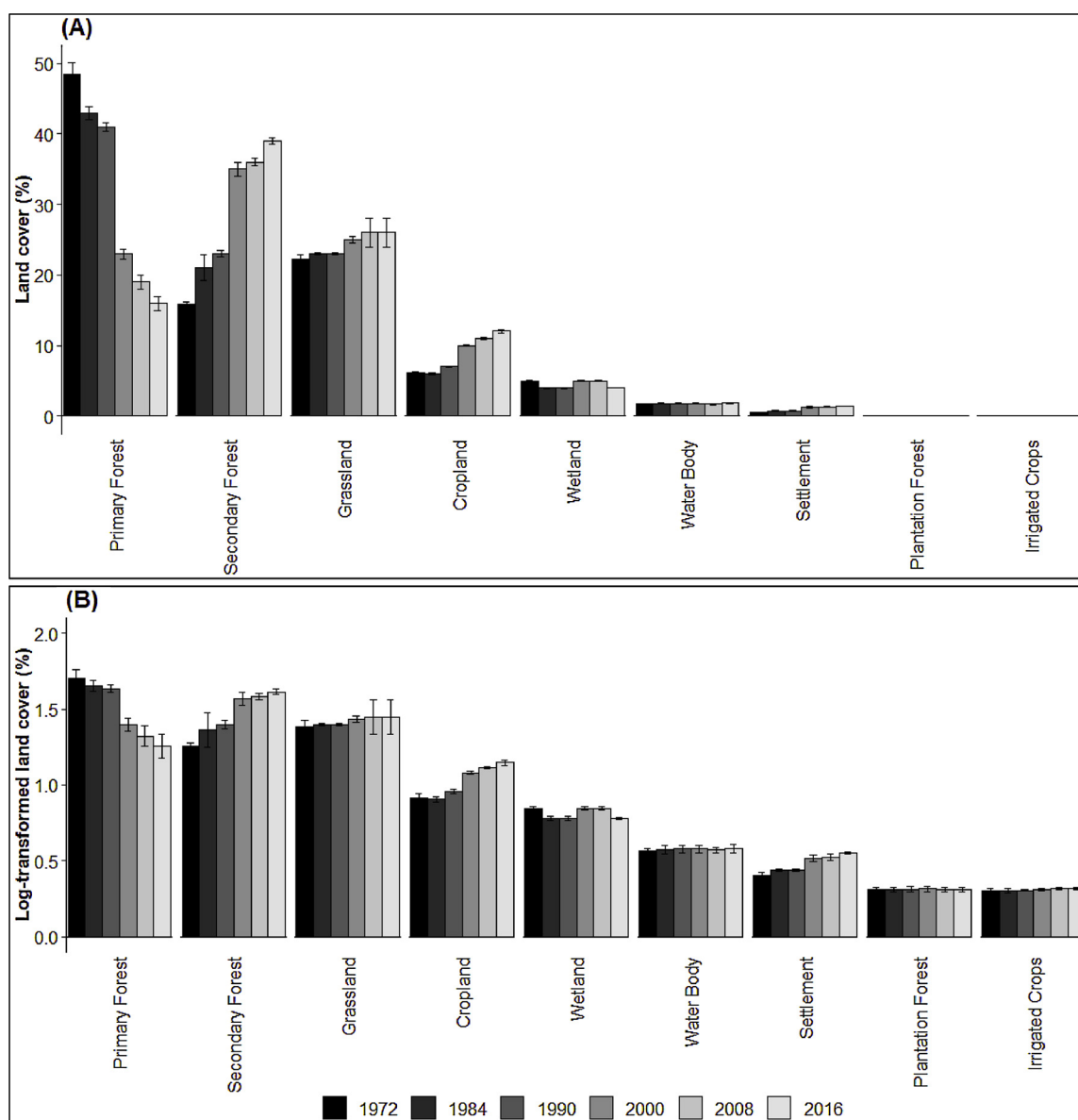
Fig. 3. (A) Land cover changes for nine different land covers and six time steps between 1972–2016. (B) Log transformed values allow for changes to be observed for land cover types with relatively small total areas (e.g. plantation forest, irrigated crops). Zambia's total area is 75.29 million ha. Error bars indicate confidence intervals.

Table 4
Land cover change transitions between 1972 and 2016. Values are in 000 s of hectares.

2016										
TO FROM	Primary Forest	Secondary Forest	Plantation Forest	Wetland	Water Body	Cropland	Irrigated Crops	Grassland	Settlement	Total Area (1972)
Primary Forest	9,557.80	16,290.50	12.40	1,130.31	68.40	3,045.08	17.20	5,929.60	284.24	36,335.52
Secondary Forest	1593.27	5,621.96	1.59	233.74	30.96	2,035.97	9.28	2,339.21	259.80	12,125.78
Plantation Forest	2.23	9.67	0.80	0.88	0.00	3.92	0.01	3.06	0.20	20.78
Wetland	273.31	1,163.51	1.16	1,021.54	83.05	208.72	3.54	986.82	12.21	3,753.85
Water Body	9.77	41.83	–	48.71	1,097.22	10.23	0.75	38.14	2.79	1,249.44
Cropland	171.83	1,566.08	0.17	60.42	13.55	1,450.60	9.93	1,284.07	83.49	4,640.15
Irrigated Crops	0.22	3.08	–	0.28	0.21	5.23	1.64	2.23	0.14	13.03
Grassland	791.87	3,956.02	0.51	508.14	70.60	2,071.30	7.65	9,258.28	83.40	16,747.77
Settlement	33.59	135.01	0.18	7.35	2.79	113.18	1.01	67.37	46.29	406.77
Total Area (2016)	12,433.89	28,787.67	16.80	3,011.36	1,366.79	8,944.22	51.02	19,908.78	772.56	75,293.09

Note that the row total sums up the amount of each land cover in the initial years (1972), while the column total sums up the amount of land cover in the final year 2016. The figures in bold on the diagonal indicate the unchanged area and the other numbers indicate the transitions. For example, the second value in the first column (1593.27) indicates the amount of secondary forest in 1972 that was converted to primary forest by 2016.

3.3. Rates of land cover change

Between 1972 and 2016, 62.74% (47 million ha) of Zambia's total land area experienced land cover change. Primary forest showed the largest decline with an annual rate of -2.48% yr^{-1} (see Supplementary Table 4). Wetland and plantation forest both declined at an annual rate of -0.50% yr^{-1}. Although irrigated crops had the smallest percentage area of the total national area (> 1% yr^{-1}), it had the highest positive rate of change of 3.20% yr^{-1} as it increased from 13,000 ha in 1972 to 51,000 ha in 2016. Secondary forest increased from 11,975,000 ha (15.80%) in 1972 to 28,993,000 ha (38.50%) in 2016 with an annual rate of change of 2.01%. Both cropland and settlement area increased at an annual rate of 1.50% yr^{-1}, with cropland increasing from 4,640,000 ha (6%) to 8,944,000 (12%) and settlement from 0.50% to 1.02% yr^{-1}. Water bodies had the lowest rate of change of 0.20% and changed from 3,753,000 ha (1.70%) in 1972 to 1,366,000 ha (1.80%) in 2016. The annual rates of change varied among the change analysis period with the period between 1990 and 2008 having the highest and the lowest rates for most land covers. For example, during this period, secondary forest and irrigated crops had the highest rates, while primary and plantation forests had the lowest rates.

3.4. Land cover transitions

Transitions between land cover classes, between 1972 and 2016, are summarised in 3. Only 30% (9,557,800 ha) of primary forests remained unchanged during the study period, with major transitions to secondary forest (net loss = 14,697,230 ha), grassland (net loss = 5,137,730 ha), and cropland (net loss = 2,873,250 ha). Meanwhile 46% (5,621,960 ha) of secondary forests in 1972 remained unchanged by 2016. In contrast to primary forests which only experienced net losses, secondary forests showed net increases against many other land covers, including primary forest, grassland (net gain = 1,616,810 ha), and wetlands (net gain = 929,770 ha). The largest net losses of secondary forest were to cropland (469,890 ha) and settlements (124,790 ha) while some areas of secondary forest also reverted to primary forests (1593,270 ha). Plantation forests were mainly established from the primary forests (net gain = 10,120 ha) and lost most of their area to secondary forest (net loss = 8080 ha) and cropland (net loss = 3750 ha).

3.4.1. Deforestation and forest degradation

Deforestation and degradation were assessed based on the losses on the three forest types. For primary and plantation forest, the losses included deforestation and degradation, while for secondary forests the losses included deforestation and regeneration to primary forest

(Fig. 4). Deforestation rates for all the forest types ranged from -0.54 to -3.05% yr^{-1} (83,000 to 453,000 ha yr^{-1}). Primary forest experienced high levels of deforestation after 1990 and deforestation for secondary forest increased between 1984 after 1990. The rates of forest degradation (conversion from primary to secondary forest) increased from - 1% yr^{-1} to - 2.23% yr^{-1} between 1990 and 2000.

3.4.2. Afforestation, regeneration and forest recovery

Afforestation and regeneration determined the gains on all the forest types, except for secondary forest, which was based on afforestation and degradation from primary forest. In this study, regeneration was defined as the change to secondary forest from areas which were once forests, while afforestation is the establishment of forests on areas which were not forests in the past. The conversion rates of non-forested areas to forests (afforestation) were between 0.01 to 1.18% yr^{-1}. Cropland (1.73 million ha), wetland (1.42 million ha) and grassland (4.75 million ha) were the major contributors towards afforestation. The highest rates of afforestation were between 1990 and 2008 with the lowest rates between 2008 and 2016 (Fig. 4). Forest regeneration ranged between 0.02% and 0.16% yr^{-1} with the highest rates between 1984 and 1990.

Forest recovery (afforestation and regeneration) rates ranged between 0.03 to 1.34% yr^{-1} (53,000 to 242,000 ha yr^{-1}) and resulted mainly from the transition of other land covers to secondary forest, regrowth to primary forest and replanting of harvested plantation areas. The forest recovery rate for the whole period was 0.25% yr^{-1} with the highest recovery of 1.07% yr^{-1} for the period 1984 to 1990. During the entire period 8.15 million ha were converted from other land covers back to forests (plantation forest = 20,170 ha, primary forest = 1.28 million ha, secondary forest = 6.86 million ha).

3.5. Forest connectivity

Fig. 5 presents the connectivity index at each classification point for primary, secondary and plantation forests, and a combination of the three forest types (all forests). The connectivity for all forests was higher than the connectivity of primary, secondary and plantation forest throughout the study period (1972–2016). The connectivity for all forests was 87% in 1972 and declined to 65% in 2016. During the initial periods (1972–1984 and 1984–1990), primary forest was more aggregated, resulting in all forests having high connectivity. The connectivity for primary forest declined throughout the whole period from 79% in 1972 to 13% in 2016, with a sharp decrease observed between 1990 and 2016. The connectivity for secondary forest increased from 16% in 1972 to 65% in 2000 before declining to 54% in 2016. A similar pattern was noticed for plantation forests with an increase in
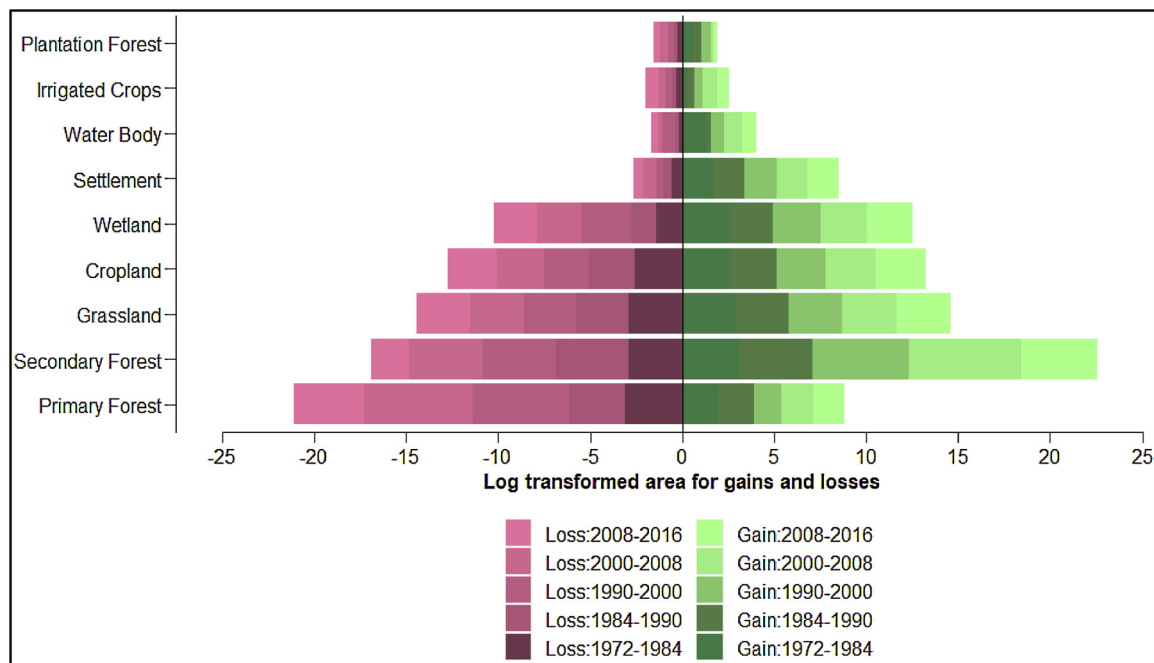
Fig. 4. Log-transformed areas for losses (left) and gains (right) for each land cover type for the six change analysis periods between 1972 and 2016. Log base 10 transformation was used on land cover areas (000 ha) to show the changes in small land covers.

connectivity from 5% in 1972 to 56% in 2000 before declining to 34% in 2016. The changes in the levels of connectivity for the classification stages was statistically different (p-value < 0.05) for the individual forests and all forests, especially on connectivity before and after 1990 (Fig. 5).

The forest connectivity was also explained indirectly by using the

number of patches (NP) and Euclidean nearest neighbour (ENN) distance. An increase in NP indicated a decline in forest connectivity and an increase in fragmentation. However, an increase in NP might also indicate a recovery of forests from other land covers. All forests showed an increase in NP throughout the classification period, except for a decline in 1990 (see Supplementary Table 6). The NP for primary forest
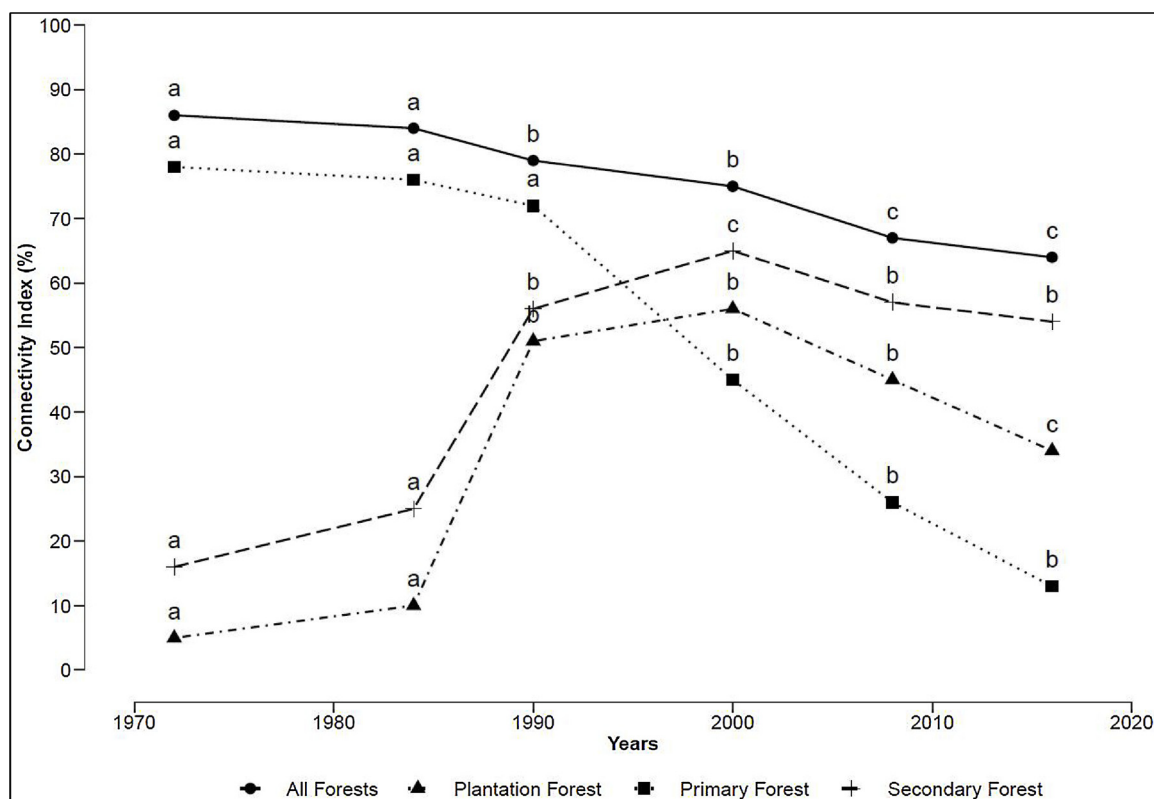

Fig. 5. The connectivity index for the forest types (primary, secondary, plantation and all forests) for six time steps between 1972 and 2016. The letters adjacent to the symbols indicate statistical differences in connectivity within each forest type.

increased between 1972 (36 million) and 1984 (41 million) and declined to 27 million in 2016. For secondary forest, the NP increased from 32 million in 1972 to 69 million in 2016; however, a decrease was noticed in 2008. For plantation forest, the number of patches increased from 56, 000 in 1972 to 196,000 in 2000 before declining to 55,000 in 2016. NP showed statistical differences (p-value < 0.05) over time for primary, secondary and plantation forest, especially for 1990–2000. The minimum distance between patches, ENN, was significantly different (p-value < 0.05) for the six classification stages for all the three types of forests and all forests (see Supplementary Table 5). The ENN for all forests increased throughout the classification from 1972 to 2016, while the ENN for secondary forest declined from 951 m in 1972 to 705 m in 2016.

4. Discussion

4.1. Land cover dynamics

The results from this study show that the wall-to-wall land cover maps for Zambia for the six time steps between 1972 and 2016 were produced with high accuracies (79 to 86%). Similar high accuracies (75–87%) were attained by Gilani et al. (2015) and Kindu et al. (2013) on Landsat imagery in Bhutan and Ethiopia, respectively. In the present study, the overall accuracies for 2000 and 2016 exceeded those for other years; this has previously been attributed to the higher spatial, spectral and radiometric resolution of the pansharpened OLI-8 and ETM + imagery (Phiri et al., 2018; Poursanidis et al., 2015). Pansharpening only improves classification accuracy and has no direct impact on change detection apart from providing accurate input for change detection, especially that post-classification change detection was employed. The lower accuracy of 79% indicates the limitation of the Landsat MSS which has a spatial resolution of 60 m; however, with an upper confidence interval of 3.79%, the accuracies were ideal for further analysis such as change detection. Compared to the available global and regional land cover maps (Chen et al., 2015; Hansen et al., 2013), this study yields greater accuracies, a long temporal record and employs relatively high-resolution datasets. Therefore, land cover maps from the present study are better suited than existing global or regional maps for national-level applications in Zambia, including forest management, land use planning and climate change programmes.

Our findings clearly show marked land cover change in Zambia between 1972 and 2016 with 62.74% of the total area experiencing change. The changes were dominated by the transition from primary to secondary forest, which is mainly attributed to degradation of intact forests resulting from the ever-increasing population, small-scale farming and unsustainable harvesting of forest products (Chomba et al., 2012; Mayes et al., 2015; Syampungani et al., 2009). This transition has previously been shown to be associated with habitat and biodiversity loss, extinction of threatened species and loss of carbon sinks (Kalacska et al., 2007; Müller et al., 2016). While causes of land cover transitions were not explored, it is possible that an increase in population, from 4 million inhabitants in 1970 to 17 million in 2017 (Simwanda and Murayama, 2017), contributed to primary forest conversion to other land cover types. Ernst et al. (2013) reported similar patterns in the decline of primary forest of the moist environment of the Congo basin, which was mainly influenced by the increasing population.

The land cover dynamics were also characterised by increasing rates of deforestation and low rates of forest recovery. Our results are in line with McNicol et al. (2018) who indicated that the rates of deforestation have remained high in sub-Saharan Africa. The rates of forest change here are higher than those reported (-0.3% yr^{-1}) by the United Nations Food and Agriculture Organisation (FAO) and are comparable to the rates of other countries in the region (e.g. Zimbabwe = -2.1 yr^{-1}, Namibia = -1.0% yr^{-1}, Uganda = -5.5% yr^{-1}) (FAO, 2015). The high rates reported in this study are because our rates were directly calculated based on remote sensing change analysis, while those reported by

FAO are usually extrapolated or based on prediction from baseline information (FAO, 2015; Morales-Hidalgo et al., 2015).

The estimates from this study are important for both FAO global forest assessment and UN-REDD + programme because of three major reasons: (1) the long historical record of over four decades, (2) the largely ignored aspect of secondary forest and forest recovery, and (3) forest degradation has been addressed through a different approach of forest connectivity. MacDicken (2015) and Morales-Hidalgo et al. (2015) indicated the challenges associated with global forest assessment information including incomplete reporting and inconsistency. The estimates of forest cover and other transitions (e.g. recovery, regeneration and degradation) in this study are consistent across different periods and hence the information is comparable. The estimates are important for updating the existing information through the forthcoming 2020 FAO Global Forest Resources Assessment Report and are applicable in exploring global drivers of change (e.g. urbanisation and population) and in the assessment of global carbon emission levels (Keenan et al., 2015; MacDicken, 2015). The present study also contributes to the monitoring of forest conditions (e.g. forest degradation) and assessing carbon credits under the UNREDD + starting from the 1990 benchmarking year. Mitchell et al. (2017) reported that assessing deforestation is much easier than assessing forest degradation in carbon assessment. Degradation has been addressed here by quantifying the transition from primary to secondary forests. Considering that the amount of carbon held by different forests types vary, the estimations of the three forest types in this study is important for stratification and carbon estimates in the specific forest types.

The decrease in primary forest cover occurred as other covers such as cropland, settlements, irrigated crops, and plantation forests increased their cover (and area). The increases in the latter land covers were likely necessary to support Zambia's increasing population. Previous studies have similarly noted the inverse relationship between forest cover, and 'anthropogenic' land covers (Chomba et al., 2012; Mayes et al., 2015; Syampungani et al., 2009). Specifically, the demand for land for agriculture and urban settlements has been found to be a major cause of significant deforestation (Reddy et al., 2016; Schulz et al., 2010). Changes in plantation forest cover were volatile during the period 1972–2016 (see Supplementary Table 5). Plantation forest cover increased between 1972 and 1990 because of the establishment of new plantations, but then declined sharply between 2000 and 2008. The continuous decline in plantation forests was mainly due to the low rates in replanting and establishment of new plantations which did not match the levels of forest harvesting driven by the demands from the mines and construction industry (Ng'andwe et al., 2015). The loss in plantation forest cover is temporary, and the area is expected to increase in the future due the plans to establish new forest plantations (Ng'andwe et al., 2015; Vinya, 2012).

An interesting result was the transition of other land covers to primary or secondary forest. This process is critical for biodiversity conservation because it indicates forest recovery due to regeneration and reversion of abandoned land covers, specifically agricultural land, to forest. Barbosa et al. (2014) indicated that secondary forests play an important role in climate change mitigation because they act as carbon sinks by storing significant amounts of carbon. Although the role of secondary forest in forest recovery after disturbance has long been acknowledged based on ground monitoring (Buttrick, 1917; Chidumayo, 2013), this had not been addressed using remotely sensed data in many dry tropical countries including Zambia. This is evident by the lack of information on primary, secondary and regenerating forest in the 2015 Global forests Assessment Report. Global studies such as Hansen et al. (2013) did not fully address forest recovery and indicated that there was no forest recovery in Zambia. However, we disagree with these findings and quantify Zambian forest recovery, which will contribute to policy formulation on afforestation and ecosystem restoration.

4.2. Forest connectivity

Assessing forest connectivity at a national scale provides critical information for monitoring forest degradation, biodiversity conservation and planning for forest management (Willcock et al., 2016; Zemanova et al., 2017). Our results indicate that the connectivity for all forests decreased by 22% between 1972 and 2016, suggesting that forests in general are becoming progressively degraded and fragmented. Similar results were reported by Echeverria et al. (2006) in the dry tropical landscape of Chile in which the connectivity decreased by 35% between 1985 and 2013; however, that study was on a smaller scale. Many previous studies (Ernst et al., 2013; Fagan et al., 2016; Haddad et al., 2015) have attributed decreases in forest connectivity to changes in land use practices, especially agricultural activities and the construction of settlements, roads or railways in forests. These factors also apply to Zambia. Since 1990, many forested areas have been degraded or deforested to make way for agriculture and infrastructure development resulting in high levels of fragmentation and low levels of connectivity for the remaining forests (Chidumayo, 2013; Mayes et al., 2015).

The connectivity for primary forest declined over the study period, while secondary and plantation forest connectivity increased. The increase in the connectivity for secondary forest was driven by the transition from primary to secondary forest. Nyamugama and Kakembo (2015) reported similar results in South Africa where the connectivity for intact forests declined, while that for degraded areas increased. Establishment of new plantation between 1984 and 2000 explains the increase in connectivity for plantation forest. Many studies have reported that forest structural connectivity and fragmentation are greatly influenced by patch isolation (Eberle et al., 2017; Nyamugama and Kakembo, 2015; Tischendorf and Fahrig, 2000). This implies that patches that are isolated have a greater chance of being completely transformed into other land covers and hence reduce forest connectivity.

The establishment of new forest plantations and implementation of conservation programmes (e.g. UN-REDD+) are likely to affect Zambia's forest connectivity in the future (De Sy et al., 2012; Vinya, 2012). In addition, sustainable methods of agriculture, which promote biodiversity conservation are being promoted through agroforestry and conservation agriculture and hence this study will act as a reference point for monitoring the impact of these conservation programmes (Syampungani et al., 2010). Going forward, these practices are likely to improve forest connectivity across the landscape of Zambia.

4.3. Implications and limitations of the study

This study presents consistent information for forest monitoring and land use planning in Zambia. The information on forest dynamics informs decision makers on where to apply effective forest management programmes, and this information will act as reference levels for future forest assessments. Our results present opportunities to consolidate information in the forthcoming FAO Global Forest Assessment Report for 2020, especially on the area covered by primary and secondary forests which were not reported in 2015 (FAO, 2015). The information will also play a vital role in climate change programmes such as the UNFCCC, Paris Agreement and Kyoto Protocol under the monitoring, reporting and verification (MRV) for the UN-REDD+. Specifically, the information will be useful for benchmarking and for estimating carbon credits in line with the IPCC Good Practices Guidelines (Birdsey et al., 2013; GOFC-GOLD, 2009). The forest connectivity results will play an important role in monitoring the success of current and future reforestation and ecosystem restoration programmes.

The results presented should be interpreted within the context of the study's limitations. Firstly, the classification accuracy was dependent upon the quality of the input images which were different across the four types of Landsat images (Table 1). Since the image quality and

properties differed across the six time steps because of the different satellite sensors used, the levels of accuracy and certainty of the results from these images vary. The variation in the levels of accuracy might also affect the results for forest connectivity. Secondly, the land cover and area values reported are snapshots in time. They describe the land cover in Zambia for six discrete time steps over the past 45 years. Consequently, land cover changes within each time step cannot be described. Capturing the nuance of ephemeral land cover changes would require increasing the number of time steps. Finally, though some drivers of land cover change were discussed above (e.g. population growth), it is acknowledged that numerous other factors contribute to land cover dynamics (Kim et al., 2014; Serneels and Lambin, 2001). Previous studies grouped the factor (drivers) of land cover change into direct and indirect factors (Chidumayo, 1989; Ernst et al., 2013; Vinya, 2012). The indirect factors include government policies, social-economic condition, demographic structures and environmental factors, while direct factors include agriculture expansion, infrastructure development, forest resource extraction and fire. A future study to comprehensively understand the drivers of change for the land cover dynamics described in the present study could inform Zambia's land use planning and policy.

5. Conclusions

We produced for the first time the empirical results of a nationwide land cover dynamics and forest connectivity analysis for Zambia, a sub-Saharan country. Our study fills the information gap on the nationwide forest losses and recovery, which have been lacking in the dry tropical environment, especially on a long temporal scale. Our findings showed increasing rates of forests decline and low levels of forest recovery. We also reported the decline in primary forest and the increase in secondary forests, which have come to dominate the landscape – a sign of both forest degradation and recovery. Other land covers such as cropland, grassland and settlements increased over the study period, while wetland and plantation forest declined. The annual rates of change of different land covers varied during the five periods of change analysis with most of the land covers having high rates of change between 1990 and 2008. Overall, forest connectivity declined by 22% between 1972 and 2016, mainly driven by a decrease in primary forest connectivity. In contrast, the connectivity for secondary and plantation forest increased due to primary forest degradation to secondary forest, reversion of abandoned agricultural land to secondary forest, and establishment of new plantation forests. The land cover estimates produced here are critical for national policies including sustainable forest management and climate change mitigation programmes such as the UNREDD+. This information will also be useful to the Zambia Forest Department for the forthcoming 2020 Global Forest Resources Assessment Report. Furthermore, the information from this study is vital for benchmarking and estimating carbon credits under the UN-REDD+ for the period 1990 to 2016.

References

Aguilar, M.A., Nemmaoui, A., Novelli, A., Aguilar, F.J., García Lorca, A.J.R.S., 2016. Object-based greenhouse mapping using very high resolution satellite data and Landsat 8 time series. Remote Sens. 8, 513. https://doi.org/10.3390/rs8060513.

Atzberger, C., Darvishzadeh, R., Immitzer, M., Schlerf, M., Skidmore, A., le Maire, G., 2015. Comparative analysis of different retrieval methods for mapping grassland leaf area index using airborne imaging spectroscopy. Int. J. Appl. Earth Obs. Geoinf. 43, 19–31. https://doi.org/10.1016/j.jag.2015.01.009.

Barbosa, J., Broadbent, E., Bitencourt, M., 2014. Remote sensing of aboveground biomass in tropical secondary forests: a review. JIRCAS J. Sci. Pap. 14. https://doi.org/10.1155/2014/715796.

Belgiu, M., Drăguţ, L., 2016. Random forest in remote sensing: a review of applications and future directions. ISPRS J. Photogramm. Remote Sens. 114, 24–31. https://doi.org/10.1016/j.isprsjprs.2016.01.011.

Bezryadin, S., Bourov, P., Ilinih, D., 2007. Brightness Calculation in Digital Image Processing. Paper Presented at the International Symposium on Technologies for Digital Photo Fulfillment. Las Vegas, USA. .

Birdsey, R., Angeles-Perez, G., Kurz, W.A., Lister, A., Olguin, M., Pan, Y., et al., 2013. Approaches to monitoring changes in carbon stocks for REDD +. Carbon Manag. 4, 519–537. https://doi.org/10.4155/cmt.13.49.

Birth, G.S., McVey, G.R., 1968. Measuring the color of growing turf with a reflectance spectrophotometer. Agron. J. 60, 640–643. https://doi.org/10.2134/agronj1968.00021962006000060016x.

Bonferroni, C., 1936. Teoria statistica delle classi e calcolo delle probabilita. Pubblicazioni del R Istituto Superiore di Scienze Economiche e Commericiali di Firenze. 8, 3–62.

Brandt, M., Wigneron, J.P., Chave, J., Tagesson, T., Penuelas, J., et al., 2018. Satellite passive microwaves reveal recent climate-induced carbon losses in African drylands. Nat. Ecol. Evol. 2, 827–835. https://www.nature.com/articles/s41559-018-0530-6.

Buttrick, P.L., 1917. Forest growth on abandoned agricultural land. Sci. Mon. 5, 80–91.

Cao, S., Yu, Q., Sanchez-Azofeifa, A., Feng, J., Rivard, B., Gu, Z., 2015. Mapping tropical dry forest succession using multiple criteria spectral mixture analysis. ISPRS J. Photogramm. Remote Sens. 109, 17–29. https://doi.org/10.1016/j.isprsjprs.2015.08.009.

Chance, C.M., Hermosilla, T., Coops, N.C., Wulder, M.A., White, J.C., 2016. Effect of topographic correction on forest change detection using spectral trend analysis of Landsat pixel-based composites. Int. J. Appl. Earth Obs. Geoinf. 44, 186–194. https://doi.org/10.1016/j.jag.2015.09.003.

Chen, J., Chen, J., Liao, A., Cao, X., Chen, L., Chen, X., et al., 2015. Global land cover mapping at 30 m resolution: a POK-based operational approach. ISPRS J. Photogramm. Remote Sens. 109 (17-29), 7–27. https://doi.org/10.1016/j.isprsjprs.2014.09.002. 103.

Chidumayo, E.N., 1989. Land use, deforestation and reforestation in the Zambian Copperbelt. Land Degrad. Dev. 1, 209–216. https://doi.org/10.1002/ldr.3400010305.

Chidumayo, E.N., 2002. Changes in miombo woodland structure under different land tenure and use systems in central Zambia. J. Biogeogr. 29, 1619–1626. https://doi.org/10.1046/j.1365-2699.2002.00794.x.

Chidumayo, E.N., 2013. Forest degradation and recovery in a miombo woodland landscape in Zambia: 22 years of observations on permanent sample plots. For. Ecol. Manage. 291, 154–161. https://doi.org/10.1016/j.foreco.2012.11.031.

Chomba, B., Tembo, O., Mutandi, K., Makano, A., 2012. Drivers of Deforestation, Identification of Threatened Forests and Forest Cobenefits Other Than Carbon from REDD+ Implementation in Zambia. A consultancy report prepared for the Forestry Department and the Food and Agriculture Organization of the United Nations under the national UN-REDD Programme. Ministry of Lands, Natural Resources and Environmental Protection, Lusaka, Zambia.

Chuvieco, E., Martin, M.P., Palacios, A., 2002. Assessment of different spectral indices in the red-near-infrared spectral domain for burned land discrimination. Int. J. Remote Sens. 23, 5103–5110. https://doi.org/10.1080/01431160210153129.

Congalton, R.G., Green, K., 2009. Assessing the Accuracy of Remotely Sensed Data: Principles and Practices, second ed. CRC Press/Taylor & Francis, Boca Raton.

De Sy, V., Herold, M., Achard, F., Asner, G.P., Held, A., Kellndorfer, J., Verbesselt, J., 2012. Synergies of multiple remote sensing data sources for REDD+ monitoring. Curr. Opin. Environ. Sustain. 4, 696–706. https://doi.org/10.1016/j.cosust.2012.09.013.

Drăguţ, L., Csillik, O., Eisank, C., Tiede, D., 2014. Automated parameterisation for multi-scale image segmentation on multiple layers. ISPRS J. Photogramm. Remote Sens. 88, 119–127. https://doi.org/10.1016/j.isprsjprs.2013.11.018.

Drăguţ, L., Tiede, D., Levick, S.R., 2010. ESP: a tool to estimate scale parameter for multiresolution image segmentation of remotely sensed data. Int. J. Geogr. Inf. Sci. 24, 859–871. https://doi.org/10.1080/13658810903174803.

Dronova, I., 2015. Object-based image analysis in wetland research: a review. Remote Sens. 7, 6380–6413. https://doi.org/10.3390/rs70506380.

Dronova, I., Gong, P., Clinton, N.E., Wang, L., Fu, W., Qi, S., Liu, Y., 2012. Landscape analysis of wetland plant functional types: the effects of image segmentation scale, vegetation classes and classification methods. Remote Sens. Environ. 127, 357–369. https://doi.org/10.1016/j.rse.2012.09.018.

Dunn, O.J., 1961. Multiple comparisons among means. J. Am. Stat. Assoc. 56, 52–64.

Eberle, J., Rödder, D., Beckett, M., Ahrens, D., 2017. Landscape genetics indicate recently increased habitat fragmentation in African forest-associated chafers. Glob. Change Biol. 23, 1988–2004. https://doi.org/10.1111/gcb.13616.

Echeverria, C., Coomes, D., Salas, J., Rey-Benayas, J.M., Lara, A., Newton, A., 2006. Rapid deforestation and fragmentation of Chilean temperate forests. Biol. Conserv. 130, 481–494. https://doi.org/10.1016/j.biocon.2006.01.017.

Ernst, C., Mayaux, P., Verhegghen, A., Bodart, C., Christophe, M., Defourny, P., 2013. National forest cover change in Congo Basin: deforestation, reforestation, degradation and regeneration for the years 1990, 2000 and 2005. Glob. Change Biol. 19, 1173–1187. https://doi.org/10.1111/gcb.12092.

ESRI, 2016. ArcGIS Descktop. Release 10.4. Relands. Environment System Research Institute., CA.

Fagan, M.E., DeFries, R.S., Sesnie, S.E., Arroyo-Mora, J.P., Chazdon, R.L., 2016. Targeted reforestation could reverse declines in connectivity for understory birds in a tropical habitat corridor. Ecol. Appl. 26, 1456–1474. https://doi.org/10.1890/14-2188.

FAO, 2015. Global Forest Resources Assesment 2015. Rome, Italy: Retrieved from. http://www.fao.org/3/a-i4808e.pdf.

Finer, M., Novoa, S., Weisse, M.J., Petersen, R., Mascaro, J., Souto, T., et al., 2018. Combating deforestation: from satellite to intervention. Science 360, 1303–1305. https://doi.org/10.1126/science.aat1203.

Gilani, H., Shrestha, H.L., Murthy, M.S.R., Phuntso, P., Pradhan, S., Bajracharya, B., Shrestha, B., 2015. Decadal land cover change dynamics in Bhutan. J. Environ. Manag. 148, 91–100. https://doi.org/10.1016/j.jenvman.2014.02.014.

Gilbertson, J.K., Kemp, J., Van Niekerk, A., 2017. Effect of pan-sharpening multi-temporal Landsat 8 imagery for crop type differentiation using different classification techniques. Comput. Electron. Agric. 134, 151–159. https://doi.org/10.1016/j.compag.2016.12.006.

Gitelson, A.A., Merzlyak, M.N., 1998. Remote sensing of chlorophyll concentration in higher plant leaves. Adv. Space Res. 22, 689–692. https://doi.org/10.1016/S0273-1177(97)01133-2.

Gitelson, Stark, R., Grits, U., Rundquist, D., Kaufman, Y., Derry, D., 2002. Vegetation and soil lines in visible spectral space: a concept and technique for remote estimation of vegetation fraction. Int. J. Remote Sens. 23, 2537–2562. https://doi.org/10.1080/01431160110107806.

GOFC-GOLD, 2009. A Sourcebook of Methods and Procedures for Monitoring and Reporting Anthropogenic Greenhouse Gas Emission and Removals Caused by Deforestation, Gains and Losses of Carbon Stocks in Forests Remaining Forest and Forestation.

Grech, A., Hanert, E., McKenzie, L., Rasheed, M., Thomas, C., Tol, S., et al., 2018. Predicting the cumulative effect of multiple disturbances on seagrass connectivity. Glob. Change Biol. 24, 3093–3104. https://doi.org/10.1111/gcb.14127.

Haddad, N.M., Brudvig, L.A., Clobert, J., Davies, K.F., Gonzalez, A., Holt, R.D., et al., 2015. Habitat fragmentation and its lasting impact on Earth's ecosystems. Sci. Adv. 1https://doi.org/10.1126/sciadv.1500052. e1500052.

Hansen, T., 2012. A review of large area monitoring of land cover change using Landsat data. Remote Sens. Environ. 122, 66–74. https://doi.org/10.1016/j.rse.2011.08.024.

Hansen, M.C., DeFries, R., Townshend, J.R., Sohlberg, R., 2000. Global land cover classification at 1 km spatial resolution using a classification tree approach. Int. J. Remote Sens. 21, 1331–1364. https://doi.org/10.1080/014311600210209.

Hansen, M.C., Potapov, P.V., Moore, R., Hancher, M., Turubanova, S.A., Tyukavina, A., et al., 2013. High-resolution global maps of 21st-Century forest cover change. Science 342, 850–853. https://doi.org/10.1126/science.1244693.

Haralick, R.M., Shanmugam, K., 1973. Textural features for image classification. IEEE Trans. Cybern. 610–621. https://doi.org/10.1109/TSMC.1973.4309314.

Henry, L.-A., Mayorga-Adame, C.G., Fox, A.D., Polton, J.A., Ferris, J.S., McLellan, F., et al., 2018. Ocean sprawl facilitates dispersal and connectivity of protected species. Sci. Rep. 8https://doi.org/10.1038/s41598-018-29575-4. 11346.

Huete, D.K., Miura, T., Rodriguez, E.P., Gao, X., Ferreira, L.G., 2002. Overview of the radiometric and biophysical performance of the MODIS vegetation indices. Remote Sens. Environ. 83, 195–213. https://doi.org/10.1016/S0034-4257(02)00096-2.

Immitzer, M., Vuolo, F., Atzberger, C., 2016. First experience with Sentinel-2 data for crop and tree species classifications in Central Europe. Remote Sens. 8, 166. https://doi.org/10.3390/rs8030166.

Kalaba, F.K., Quinn, C.H., Dougill, A.J., Vinya, R., 2013. Floristic composition, species diversity and carbon storage in charcoal and agriculture fallows and management implications in Miombo woodlands of Zambia. For. Ecol. Manage. 304, 99–109. https://doi.org/10.1016/j.foreco.2013.04.024.

Kalacska, M., Sanchez-Azofeifa, G.A., Rivard, B., Caelli, T., White, H.P., Calvo-Alvarado, J.C., 2007. Ecological fingerprinting of ecosystem succession: estimating secondary tropical dry forest structure and diversity using imaging spectroscopy. Remote Sens. Environ. 108, 82–96. https://doi.org/10.1016/j.rse.2006.11.007.

Keenan, R.J., Reams, G.A., Achard, F., de Freitas, J.V., Grainger, A., Lindquist, E., 2015. Dynamics of global forest area: results from the FAO global forest resources assessment 2015. For. Ecol. Manage. 352, 9–20.

Key, C., Benson, N., 2005. Landscape Assessment: Remote Sensing of Severity, the Normalized Burn Ratio and Ground Measure of Severity, the Composite Burn Index. FIREMON: Fire Effects Monitoring and Inventory System Ogden. USDA Forest Service, Rocky Mountain Res. Station, Utah.

Kim, I., Le, Q.B., Park, S.J., Tenhunen, J., Koellner, T., 2014. Driving forces in archetypical land-use changes in a mountainous watershed in East Asia. Land 3, 957–980. https://doi.org/10.3390/land3030957.

Kindu, M., Schneider, T., Teketay, D., Knoke, T., 2013. Land use/land cover change analysis using object-based classification approach in Munessa-Shashemene landscape of the ethiopian highlands. Remote Sens. 5, 2411–2435. https://doi.org/10.3390/rs5052411.

Kruskal, W.H., 1953. Errata for Kruskal–Wallis. J. Am. Stat. Assoc. 48, 907–911 https://doi.org/https://www.jstor.org/stable/i314143.

Lebourgeois, V., Dupuy, S., Vintrou, É., Ameline, M., Butler, S., Bégué, A., 2017. A combined random forest and OBIA classification scheme for mapping smallholder agriculture at different nomenclature levels using multisource data (simulated Sentinel-2 time series, VHRS and DEM). Remote Sens. 9, 259. https://doi.org/10.3390/rs9030259.

Leventon, J., Kalaba, F.K., Dyer, J.C., Stringer, L.C., Dougill, A.J., 2014. Delivering community benefits through REDD+: Lessons from Joint Forest Management in Zambia. For. Policy Econ. 44, 10–17. https://doi.org/10.1016/j.forpol.2014.03.005.

MacDicken, K.G., 2015. Global forest resources assessment 2015: what, why and how? For. Ecol. Manage. 352, 3–8. https://doi.org/10.1016/j.foreco.2015.02.006.

Mayes, M.T., Mustard, J.F., Melillo, J.M., 2015. Forest cover change in Miombo Woodlands: modeling land cover of African dry tropical forests with linear spectral mixture analysis. Remote Sens. Environ. 165, 203–215. https://doi.org/10.1016/j.rse.2015.05.006.

Mc Garigal, Cushman, S.A., Ene, E., 2012. FRAGSTATS v4: Spatial Pattern Analysis Program for Categorical and Continuous Maps. Computer Software Program Produced by the Authors at the University of Massachusetts. Amherst http://www.umass.edu/landeco/research/fragstats/fragstats.html.

McNicol, I.M., Ryan, C.M., Mitchard, E.T.A., 2018. Carbon losses from deforestation and widespread degradation offset by extensive growth in African woodlands. Nat. Commun. 9, 3045. https://doi.org/10.1038/s41467-018-05386-z.

Mitchell, A.L., Rosenqvist, A., Mora, B., 2017. Current remote sensing approaches to monitoring forest degradation in support of countries measurement, reporting and verification (MRV) systems for REDD+. Carbon Balance Manag. 12 (1), 9. https://doi.org/10.1186/s13021-017-0078-9.

Morales-Hidalgo, D., Oswalt, S.N., Somanathan, E., 2015. Status and trends in global primary forest, protected areas, and areas designated for conservation of biodiversity from the Global Forest Resources Assessment 2015. For. Ecol. Manage. 352, 68–77. https://doi.org/10.1016/j.foreco.2015.06.011.

Mukosha, J.S.A., 2008. Intergrated Land Use Assesment (ILUA) Zambia. pp. 2005–2008.

Müller, H., Rufin, P., Griffiths, P., de Barros Viana Hissa, L., Hostert, P., 2016. Beyond deforestation: differences in long-term regrowth dynamics across land use regimes in southern Amazonia. Remote Sens. Environ. 186, 652–662. https://doi.org/10.1016/j.rse.2016.09.012.

Munyati, C., 2000. Wetland change detection on the Kafue Flats, Zambia, by classification of a multitemporal remote sensing image dataset. Int. J. Remote Sens. 21, 1787–1806. https://doi.org/10.1080/014311600209742.

Myint, S.W., Gober, P., Brazel, A., Grossman-Clarke, S., Weng, Q., 2011. Per-pixel vs. Object-based classification of urban land cover extraction using high spatial resolution imagery. Remote Sens. Environ. 115, 1145–1161. https://doi.org/10.1016/j.rse.2010.12.017.

Ng'andwe, P., Mwitwa, J., Muimba-Kankolongo, A., 2015. Forest Policy, Economics, and Markets in Zambia. Academic Press.

Nyamugama, A., Kakembo, V., 2015. Monitoring land cover changes and fragmentation dynamics in the subtropical thicket of the Eastern Cape Province, South Africa. South Afr. J. Geom. 4, 397–413. https://doi.org/10.4314/sajg.v4i4.4.

Olofsson, P., Foody, G.M., Herold, M., Stehman, S.V., Woodcock, C.E., Wulder, M.A., 2014. Good practices for estimating area and assessing accuracy of land change. Remote Sens. Environ. 148, 42–57. https://doi.org/10.1016/j.rse.2014.02.015.

Petit, C., Scudder, T., Lambin, E., 2001. Quantifying processes of land-cover change by remote sensing: resettlement and rapid land-cover changes in south-eastern Zambia. Int. J. Remote Sens. 22, 3435–3456. https://doi.org/10.1080/01431160010006881.

Phiri, D., Morgenroth, J., 2017. Developments in Landsat land cover classification methods: a review. Remote Sens. 9, 967. https://doi.org/10.3390/rs9090967.

Phiri, D., Phiri, E., Kasubika, R., Zulu, D., Lwali, C., 2016. The implication of using a fixed form factor in areas under different rainfall and soil conditions for Pinus kesiya in Zambia. South. For. 78, 35–39. https://doi.org/10.2989/20702620.2015.1108614.

Phiri, D., Morgenroth, J., Xu, C., Hermosilla, T., 2018. Effects of pre-processing methods on Landsat OLI-8 land cover classification using OBIA and random forests classifier. Int. J. Appl. Earth Obs. Geoinf. 73, 170–178. https://doi.org/10.1016/j.jag.2018.06.014.

Piquer-Rodríguez, M., Torella, S., Gavier-Pizarro, G., Volante, J., Somma, D., Ginzburg, R., Kuemmerle, T., 2015. Effects of past and future land conversions on forest connectivity in the Argentine Chaco. Landsc. Ecol. 30, 817–833. https://doi.org/10.1007/s10980-014-0147-3.

Poursanidis, D., Chrysoulakis, N., Mitraka, Z., 2015. 3//). Landsat 8 vs. Landsat 5: A comparison based on urban and peri-urban land cover mapping. Int. J. Appl. Earth Obs. Geoinf. 35 (Part B), 259–269. https://doi.org/10.1016/j.jag.2014.09.010.

Puyravaud, J.P., 2003. Standardizing the calculation of the annual rate of deforestation. For. Ecol. Manage. 177, 593–596. https://doi.org/10.1016/S0378-1127(02)00335-3.

R Core Team, 2013. R: a Language and Environment for Statistical Computing.

Reddy, C.S., Satish, K.V., Jha, C.S., Diwakar, P.G., Murthy, Y.V.N.K., Dadhwal, V.K., 2016. Development of deforestation and land cover database for Bhutan (1930–2014). Environ. Monit. Assess. 188 (658). https://doi.org/10.1007/s10661-016-5676-6.

Rodriguez-Galiano, V.F., Ghimire, B., Rogan, J., Chica-Olmo, M., Rigol-Sanchez, J.P., 2012. An assessment of the effectiveness of a random forest classifier for land-cover classification. ISPRS J. Photogramm. Remote Sens. 67, 93–104. https://doi.org/10.1016/j.isprsjprs.2011.11.002.

Schulz, J.J., Cayuela, L., Echeverria, C., Salas, J., Rey Benayas, J.M., 2010. Monitoring land cover change of the dryland forest landscape of Central Chile (1975–2008). Appl. Geogr. 30, 436–447. https://doi.org/10.1016/j.apgeog.2009.12.003.

Serneels, S., Lambin, E.F., 2001. Proximate causes of land-use change in Narok District, Kenya: a spatial statistical model. Agric. Ecosyst. Environ. 85, 65–81. https://doi.org/10.1016/S0167-8809(01)00188-8.

Silleos, N.G., Alexandridis, T.K., Gitas, I.Z., Perakis, K., 2006. Vegetation indices: advances made in biomass estimation and vegetation monitoring in the last 30 years. Geocarto Int. 21, 21–28. https://doi.org/10.1080/10106040608542399.

Simwanda, M., Murayama, Y., 2017. Integrating geospatial techniques for urban land use classification in the developing sub-Saharan African city of Lusaka, Zambia. ISPRS Int. J. Geoinf. 6, 102. https://doi.org/10.3390/ijgi6040102.

Syampungani, S., Chirwa, P.W., Akinnifesi, F.K., Sileshi, G., Ajayi, O.C., 2009. The Miombo Woodlands at the Cross Roads: Potential Threats, Sustainable Livelihoods, Policy Gaps and Challenges. Paper Presented at the Natural Resources Forum.

Syampungani, S., Chirwa, P.W., Akinnifesi, F.K., Ajayi, O.C., 2010. The potential of using agroforestry as a win-win solution to climate change mitigation and adaptation and meeting food security challenges in Southern Africa. Agric. J. 5, 80–88 https://doi.org/http://docsdrive.com/80-88.pdf.

Syampungani, S., Geldenhuys, C.J., Chirwa, P.W., 2016. Regeneration dynamics of miombo woodland in response to different anthropogenic disturbances: forest characterisation for sustainable management. Agrofor. Syst. 90, 563–576 https://doi.org/https://doi.org/0.1007/s10457-015-9841-7.

Tischendorf, L., Fahrig, L., 2000. How should we measure landscape connectivity? Landsc. Ecol. 15, 633–641.

Tucker, C.J., 1979. Red and photographic infrared linear combinations for monitoring vegetation. Remote Sens. Environ. 8, 127–150. https://doi.org/10.1016/0034425779)90013-0.

Uddin, K., Shrestha, H.L., Murthy, M.S.R., Bajracharya, B., Shrestha, B., Gilani, H., et al., 2015. Development of 2010 national land cover database for the Nepal. J. Environ. Manag. 148, 82–90. https://doi.org/10.1016/j.jenvman.2014.07.047.

Vanonckelen, S., Lhermitte, S., Van Rompaey, A., 2013. The effect of atmospheric and topographic correction methods on land cover classification accuracy. Int. J. Appl. Earth Obs. Geoinf. 24, 9–21. https://doi.org/10.1016/j.jag.2013.02.003.

Vinya, R., 2012. Preliminary Study on the Drivers of Deforestation and Potential for REDD+ in Zambia. A Consultancy Report Prepared for Forestry Department and FAO Under the National UN-REDD+ Programme Ministry of Lands & Natural Resources. Lusaka Zambia. .

Wieland, M., Pittore, M., 2014. Performance evaluation of machine learning algorithms for urban pattern recognition from multi-spectral satellite images. Remote Sens. 6, 2912–2939. https://doi.org/10.3390/rs6042912.

Willcock, S., Phillips, O.L., Platts, P.J., Swetnam, R.D., Balmford, A., Burgess, N.D., et al., 2016. Land cover change and carbon emissions over 100 years in an A frican biodiversity hotspot. Glob. Change Biol. 22, 2787–2800. https://doi.org/10.1111/gcb.13218.

Woodcock, C.E., Allen, R., Anderson, M., Belward, A., Bindschadler, R., Cohen, W., et al., 2008. Free access to landsat imagery. Science 320 https://doi.org/10.1126/science.320.5879.1011a. 1011-1011.

Young, N.E., Anderson, R.S., Chignell, S.M., Vorster, A.G., Lawrence, R., Evangelista, P.H., 2017. A survival guide to Landsat preprocessing. Ecology 98, 920–932. https://doi.org/10.1002/ecy.1730.

Zemanova, M.A., Perotto-Baldivieso, H.L., Dickins, E.L., Gill, A.B., Leonard, J.P., Wester, D.B., 2017. Impact of deforestation on habitat connectivity thresholds for large carnivores in tropical forests. Ecol. Process. 6 (21). https://doi.org/10.1186/s13717-017-0089-1.